

April 5, 2011

*Supporting Information for*

**Theoretical Unimolecular Kinetics for  $\text{CH}_4 + \text{M} \rightleftharpoons \text{CH}_3 + \text{H} + \text{M}$  in  
Eight Baths,  $\text{M} = \text{He, Ne, Ar, Kr, H}_2, \text{CO, N}_2, \text{ and CH}_4$**

Ahren W. Jasper and James A. Miller

*Combustion Research Facility, Sandia National Laboratories, PO Box  
969, Livermore, CA 94551-0969, USA*

- p. 2 Table S-1. Fitted intermolecular potential energy surface parameters
- 3 Fig S-1. Pictures representative of the three  $\text{CH}_4 + \text{Rg}$  approaches
- 4 Fig S-2. Interaction energies for  $\text{CH}_4 + \text{He}$
- 5 Fig S-3. Interaction energies for  $\text{CH}_4 + \text{Ne}$
- 6 Fig S-4. Interaction energies for  $\text{CH}_4 + \text{Ar, Kr}$
- 7 Fig S-5. Interaction energies for  $\text{CH}_4 + \text{CH}_4$
- 8 Fig S-6. Interaction energies for  $\text{CH}_4 + \text{H}_2$
- 9 Fig S-7. Interaction energies for  $\text{CH}_4 + \text{H}_2$
- 10 Fig S-8. Interaction energies for  $\text{CH}_4 + \text{N}_2$
- 11 Fig S-9. Interaction energies for  $\text{CH}_4 + \text{CO}$

**Table S-1. Fitted intermolecular potential energy surface parameters**

| <i>Lennard-Jones parameters (eq 23)</i> |        |      |                               |                  |                 |                 |
|---|--------|------|-------------------------------|------------------|-----------------|-----------------|
| M                                       | Fit    | Pair | $D, \text{cm}^{-1}$           | $R', \text{\AA}$ |                 |                 |
| He                                      | A      | He-H | 18.1                          | 2.91             |                 |                 |
|   |        | He-C | 80.0                          | 2.66             |                 |                 |
|   | B      | He-H | 6.51                          | 2.86             |                 |                 |
|   |        | He-C | 15.9                          | 3.16             |                 |                 |
| <i>exp/6 parameters (eq 24)</i>         |        |      |                               |                  |                 |                 |
| M                                       | Fit    | Pair | $\log_{10}(A/\text{cm}^{-1})$ | $B, \text{\AA}$  | $C, \text{\AA}$ | $S, \text{\AA}$ |
| He                                      | –      | He-H | 7.550                         | 0.2522           | 4.510           |                 |
|   |        | He-C | 6.714                         | 0.2884           | 6.167           |                 |
| Ne                                      | –      | Ne-H | 6.391                         | 0.2621           | 5.749           |                 |
|   |        | Ne-C | 7.500                         | 0.2391           | 4.802           |                 |
| Ar <sup>a</sup>                         | –      | Ar-H | 6.602                         | 0.2954           | 2.684           |                 |
|   |        | Ar-C | 7.529                         | 0.2772           | 2.663           |                 |
| Kr <sup>a</sup>                         | –      | Kr-H | 6.682                         | 0.3088           | 2.922           |                 |
|   |        | Kr-C | 7.597                         | 0.2841           | 2.540           |                 |
| H <sub>2</sub>                          | RP     | H-H  | 4.912                         | 0.3865           | 6.270           | 2.500           |
|   |        | H-C  | 5.140                         | 0.4285           | 3.250           | 2.941           |
|   | R      | H-H  | 5.239                         | 0.3176           | 5.539           | 2.625           |
|   |        | H-C  | 6.916                         | 0.2244           | 5.475           | 2.460           |
|   | P      | H-H  | 5.681                         | 0.2772           | 5.453           | 2.553           |
|   |        | H-C  | 6.250                         | 0.2896           | 1.516           | 3.000           |
| N <sub>2</sub>                          | RP     | N-H  | 6.528                         | 0.2759           | 6.459           | 0.9430          |
|   |        | N-C  | 7.145                         | 0.2861           | 0.02881         | 6.057           |
|   | R      | N-H  | 6.351                         | 0.2735           | 0.01758         | 8.710           |
|   |        | N-C  | 6.750                         | 0.3008           | 8.438           | 2.849           |
|   | P      | N-H  | 6.500                         | 0.2600           | 4.496           | 3.099           |
|   |        | N-C  | 7.438                         | 0.2652           | 8.188           | 3.050           |
| CO                                      | RP     | C-H  | 7.127                         | 0.2261           | 6.562           | 3.285           |
|   |        | C-C  | 7.500                         | 0.2763           | 1.681           | 7.134           |
|   |        | O-H  | 5.000                         | 0.3990           | 2.000           | 2.458           |
|   |        | O-C  | 6.000                         | 0.3399           | 8.750           | 3.001           |
|   |        |      |                               |                  |                 |                 |
|   | R O-in | C-H  | 6.680                         | 0.2922           | 0.7389          | 1.451           |
|   |        | C-C  | 7.188                         | 0.2389           | 8.748           | 2.501           |
|   |        | O-H  | 5.000                         | 0.4131           | 0.9066          | 8.748           |
|   |        | O-C  | 6.937                         | 0.3032           | 8.985           | 2.293           |
|   |        |      |                               |                  |                 |                 |

<sup>a</sup>From Alexander; W. A.; Troya, D. *J. Phys. Chem.* **2006**, *110*, 10834.

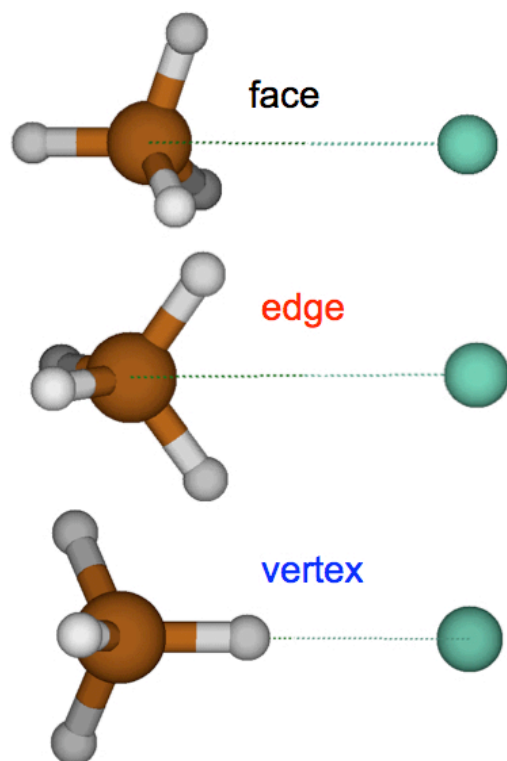
**Figure S-1**

Fig. S-1. Representations of the three approaches considered for the atomic baths.

Figure S-2

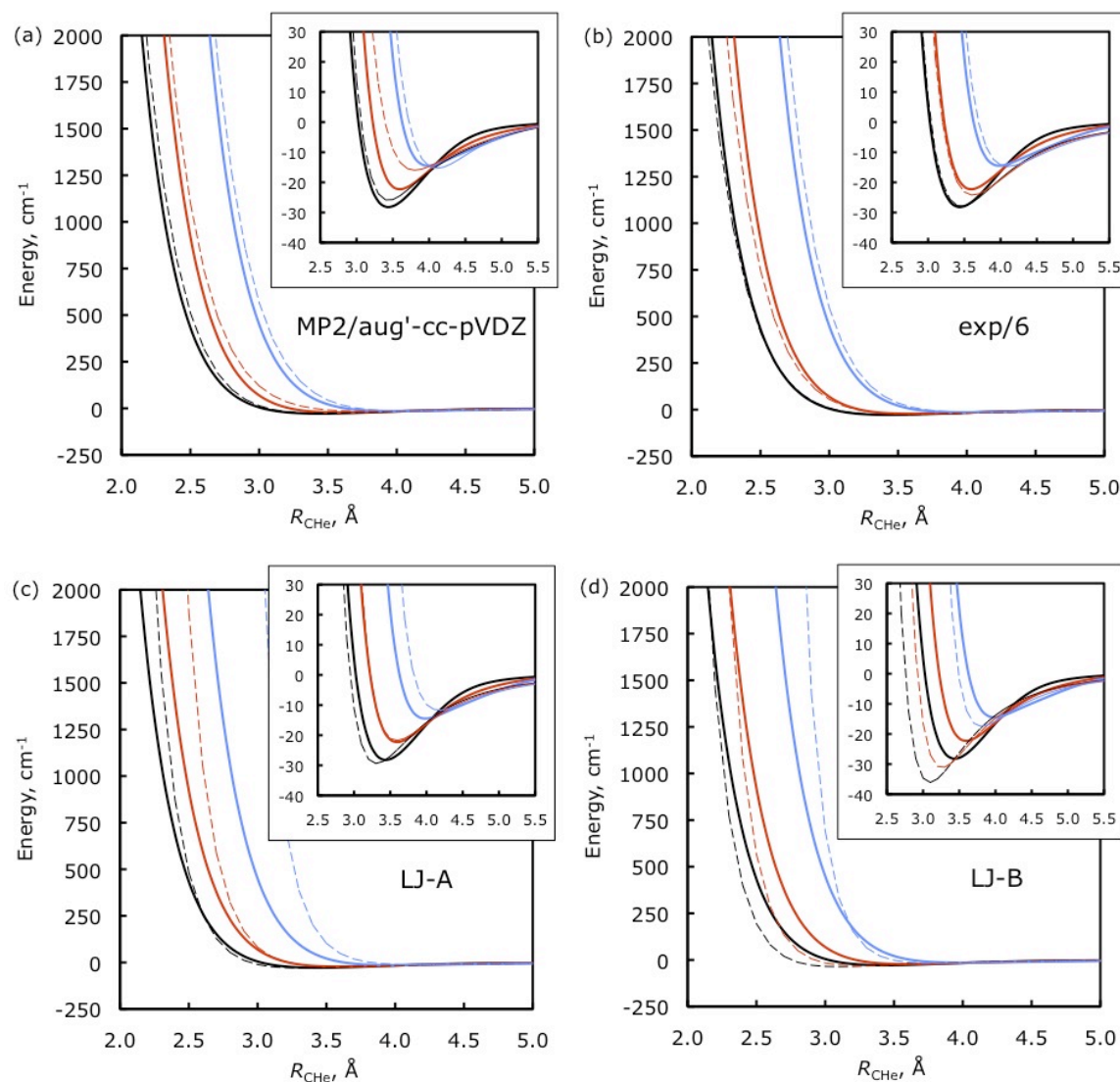


Fig. S-2 (Fig. 1 in the article)  $\text{CH}_4 + \text{He}$  interaction potential for face (black), edge (red), and vertex (blue) approaches. The solid lines in all four panels are QCISD(T)/CBS energies, and the dashed lines are (a) MP2/aug'-cc-pVDZ, (b) exp/6, (c) LJ-A, and (d) LJ-B energies. The insets highlight the van der Waals wells.

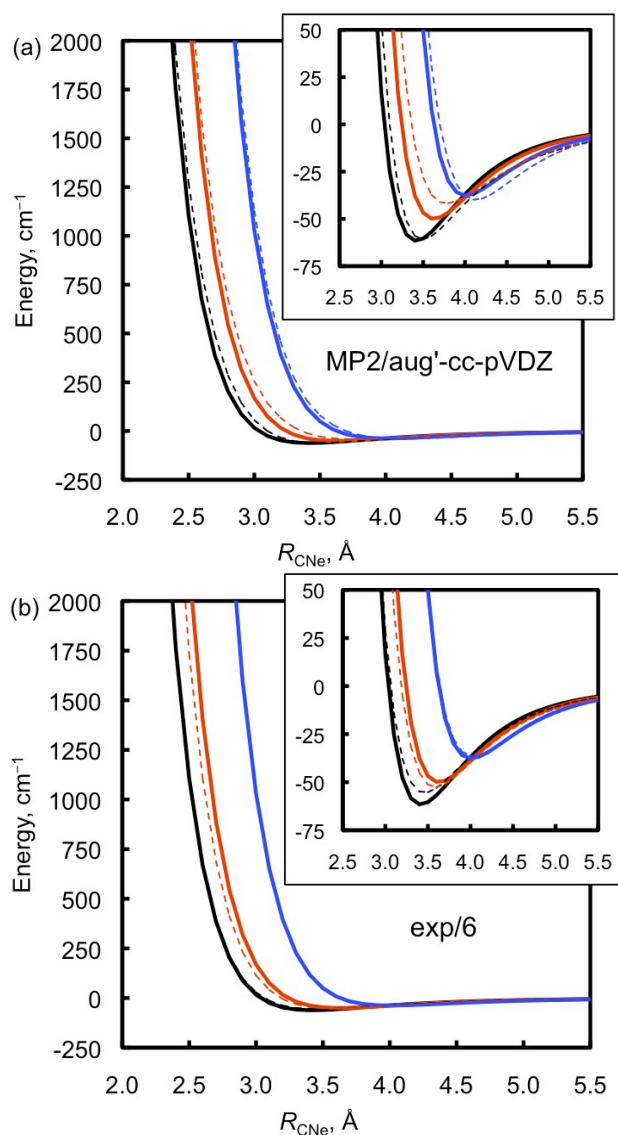
**Figure S-3**

Fig. S-3 Comparison of the QCISD(T)/CBS  $\text{CH}_4 + \text{Ne}$  interaction potential along three approaches (solid) with those for the (a) MP2/aug'-cc-pVDZ and (b) exp/6 methods (dashed). The color code for the approaches is the same as in Fig. S-2.

Figure S-4

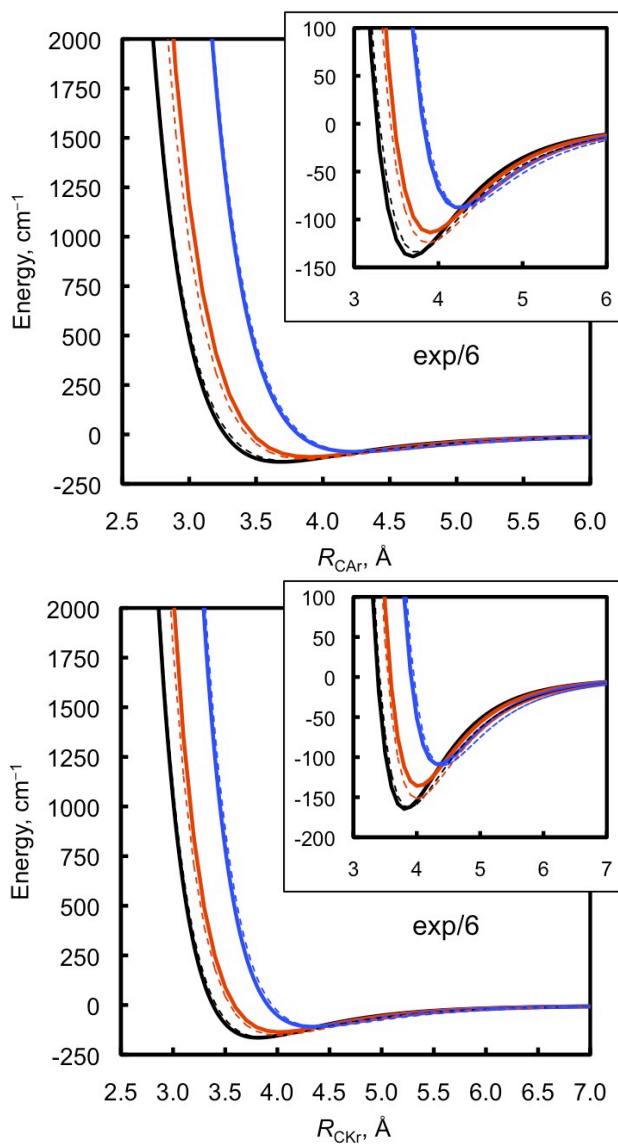


Fig. S-4 Comparison of the QCISD(T)/CBS  $\text{CH}_4 + \text{M}$  interaction potential (solid) along three approaches with those for the exp/6 method (dashed) for (a) Ar and (b) Kr. The color code for the approaches is the same as in Fig. S-2.

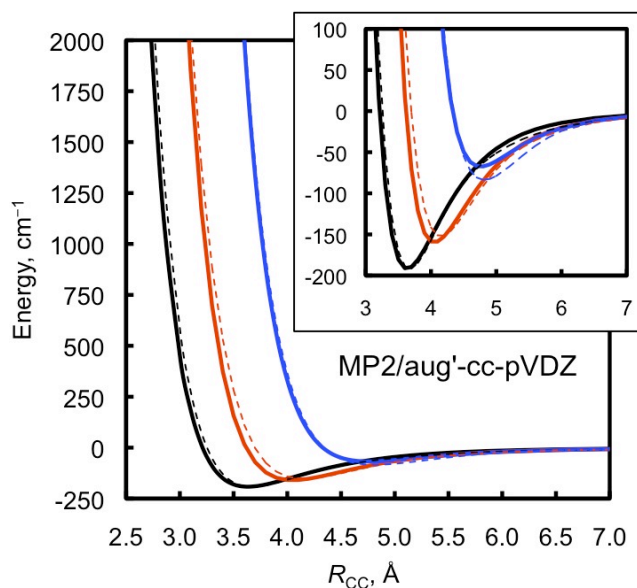
**Figure S-5**

Fig. S-5 Comparison of the QCISD(T)/CBS  $\text{CH}_4 + \text{CH}_4$  interaction potential (solid) along three approaches (black: face-face, red: face-vertex, blue: vertex-vertex) with those for the MP2/aug'-cc-pVDZ method (dashed).

Figure S-6

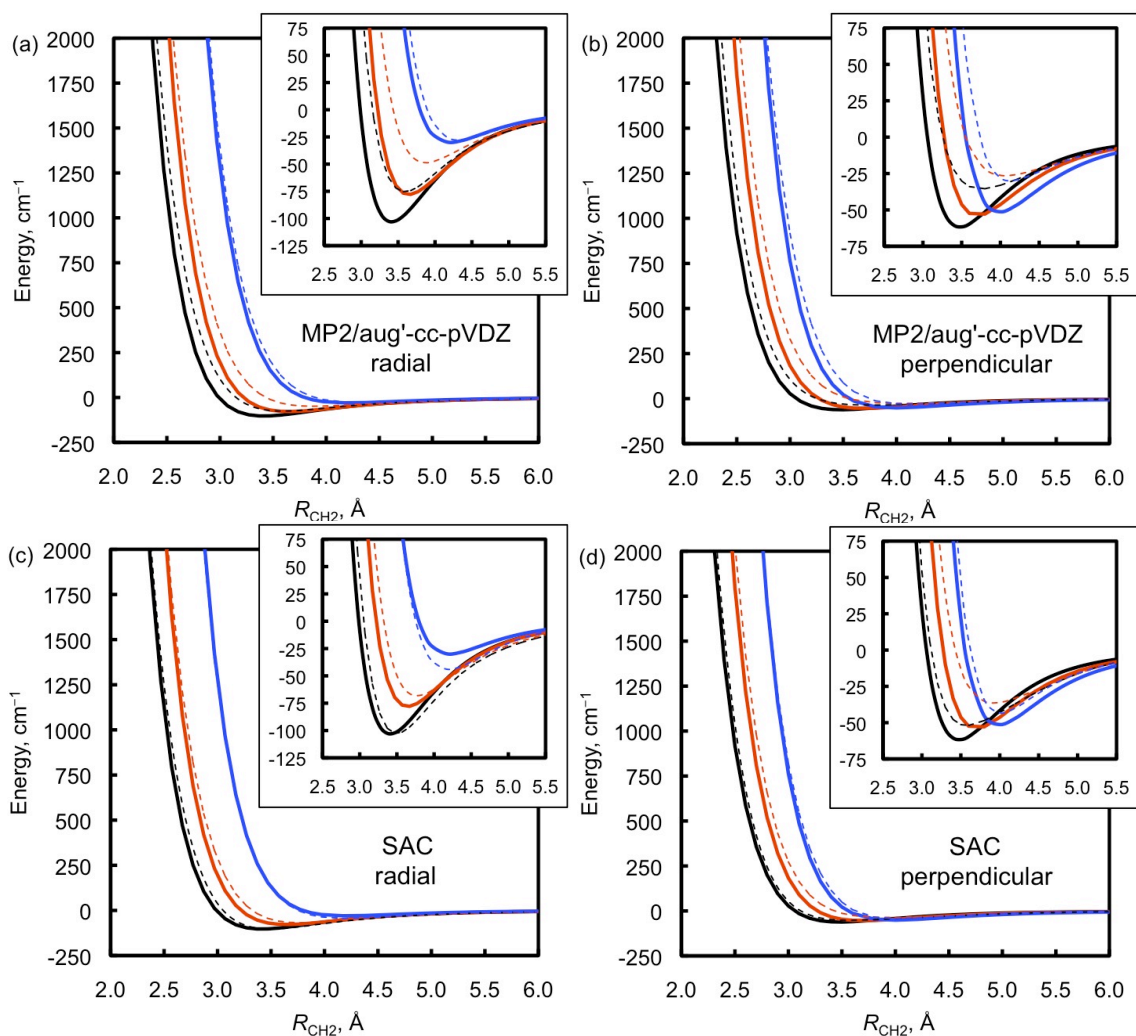


Fig. S-6 Comparison of the QCISD(T)/CBS  $\text{CH}_4 + \text{H}_2$  interaction potential (solid) along six approaches with those for the (a,b) MP2/aug'-cc-pVDZ and (c,d) SAC/aug'-cc-pVDZ methods (dashed). The color code for the approaches is the same as in Fig. S-2.  $\text{H}_2$  is aligned in the direction of the approach (radially) in (a,c) and perpendicular to the direction of approach in (b,d).



Figure S-7

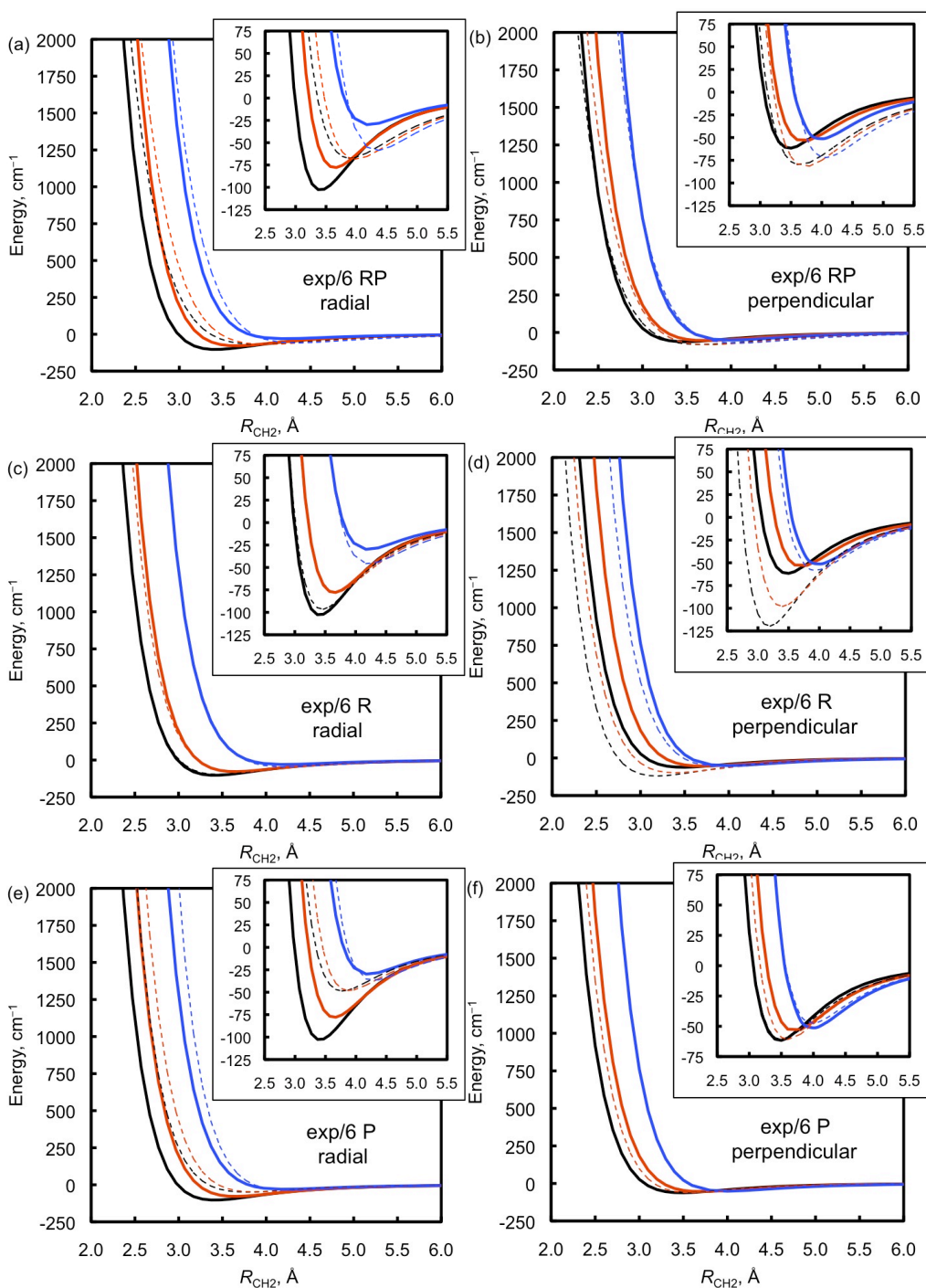


Fig. S-7 (Fig. 2 in the article) Comparison of the QCISD(T)/CBS  $\text{CH}_4 + \text{H}_2$  interaction potential (solid) along six approaches with the exp/6 method for the (a,b) compromise (RP), (c,d) radial-only (R), and (e,f) perpendicular-only (P) fits (dashed). The color code for the approaches is the same as in Fig. S-2.  $\text{H}_2$  is aligned in the direction of the approach (radially) in (a,c,e) and perpendicularly in (b,d,f).

Figure S-8

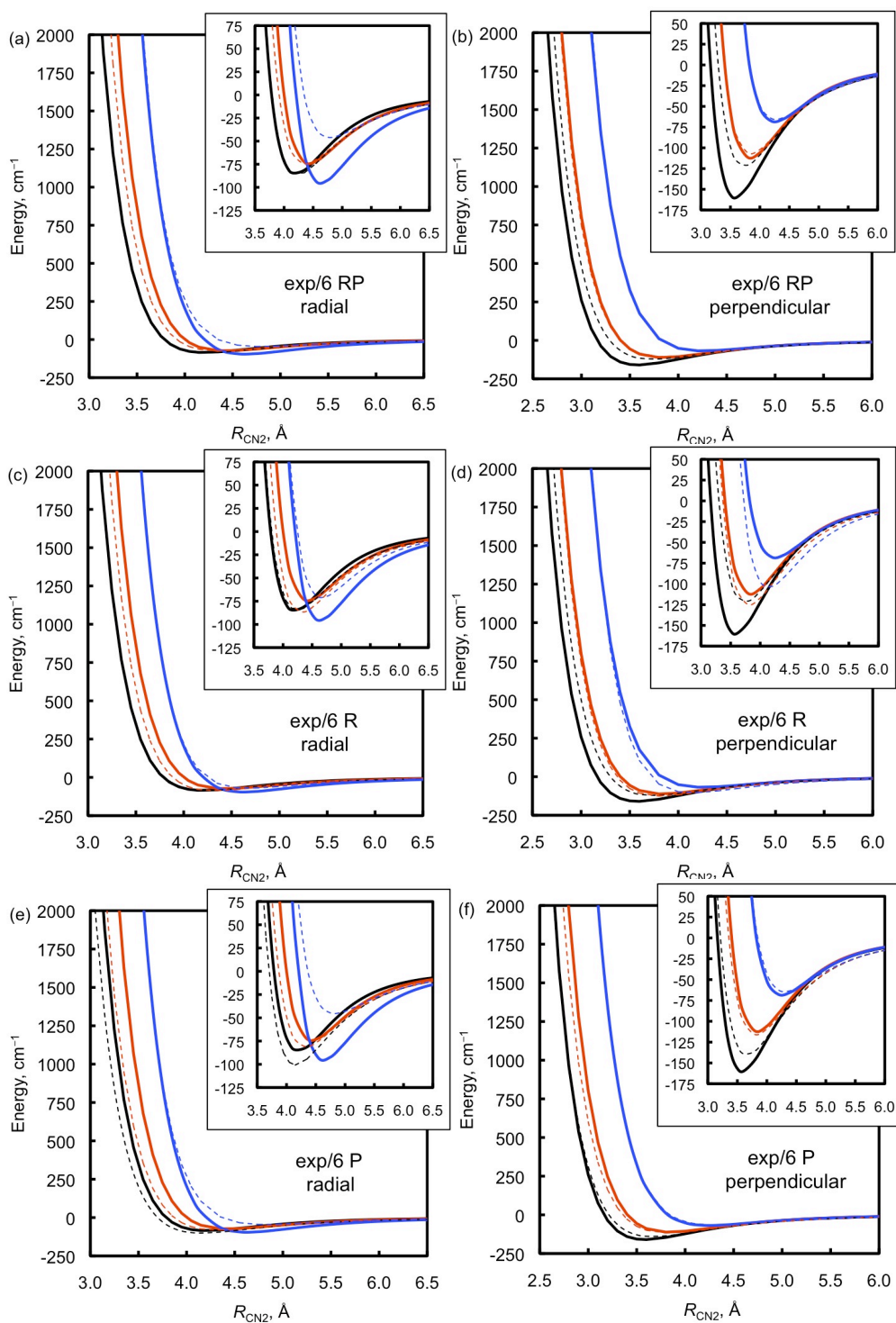


Fig. S-8 Comparison of the QCISD(T)/CBS  $\text{CH}_4 + \text{N}_2$  interaction potential (solid) along six approaches with the exp/6 method for the (a,b) compromise (RP), (c,d) radial-only (R), and (e,f) perpendicular-only (P) fits (dashed). The color code for the approaches is the same as in Fig. S-2.  $\text{N}_2$  is aligned in the direction of the approach (radially) in (a,c,e) and perpendicularly in (b,d,f).

Figure S-9

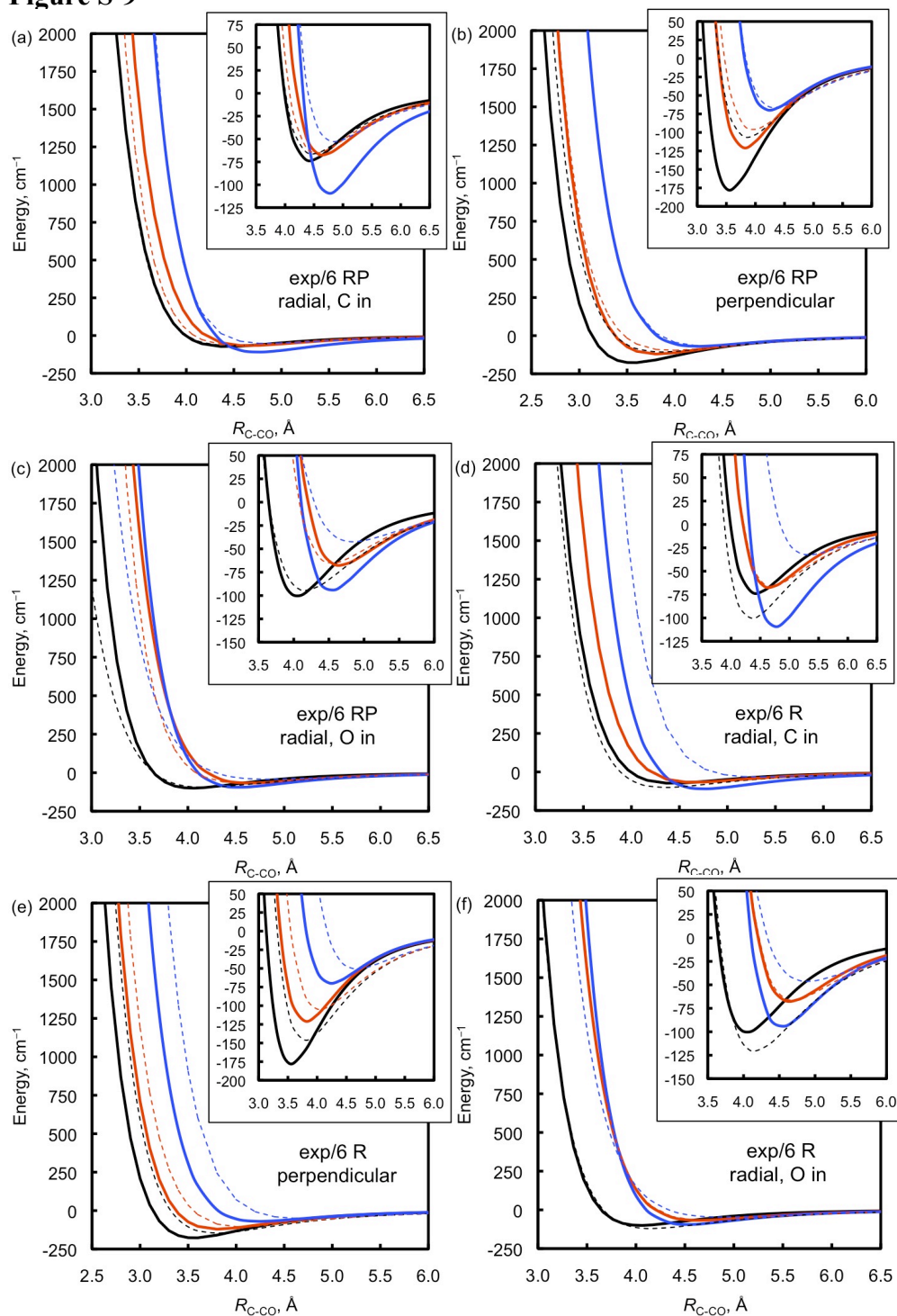


Fig. S-9 Comparison of the QCISD(T)/CBS  $\text{CH}_4 + \text{CO}$  interaction potential (solid) along nine approaches with the exp/6 method for the (a,b,c) compromise (RP) and (d,e,f) O-in radial-only (R) fits (dashed). The color code for the approaches is the same as in Fig. S-2. CO is aligned in the direction of the approach (radially) with C facing  $\text{CH}_4$  in (a,d), perpendicularly in (b,e), and radially with O approaching  $\text{CH}_4$  in (c,f).